Proc. Natl. Acad. Sci. USA
Vol. 92, pp. 97–101, January 1995
Biophysics

Conformational implications of asparagine-linked glycosylation

BARBARA IMPERIALI* AND KEITH W. RICKERT

Division of Chemistry and Chemical Engineering, California Institute of Technology, Pasadena, CA 91125

Communicated by Peter B. Dervan, California Institute of Technology, Pasadena, CA, September 20, 1994 (received for review June 23, 1994)

ABSTRACT **The effects of cotranslational protein modification on the process of protein folding are poorly understood. Time-resolved fluorescence energy transfer has been used to assess the impact of glycosylation on the conformational dynamics of flexible oligopeptides. The peptide sequences examined are selected from glycoproteins of known three-dimensional structure. The energy transfer modulation associated with N-linked glycosylation is consistent with the glycopeptides sampling different conformational profiles in water. Results show that glycosylation causes the modified peptides to adopt a different ensemble of conformations, and for some peptides this change may lead to conformations that are more compact and better approximate the conformation of these peptides in the final folded protein. This result further implies that cotranslational glycosylation can trigger the timely formation of structural nucleation elements and thus assist in the complex process of protein folding.**

The synthesis of many proteins takes place on membrane-associated ribosomes and follows the secretory pathway (1). These proteins are subject to a wide array of enzyme-catalyzed covalent chemical modifications. Early protein modification reactions, such as glycosylation, carboxylation, and hydroxylation, occur on protein substrates that are either only locally folded or in the form of "collapsed intermediates" (2). Because these protein processing events occur cotranslationally, questions arise as to the impact of each modification on the local peptide conformation and on the progress and efficiency of subsequent protein-folding events. Numerous observations attest to the importance of asparagine glycosylation for the appropriate folding and assembly of intact proteins. For example, the biosynthesis of proteins in the presence of N-linked glycosylation inhibitors, such as tunicamycin, often results in extensive aggregation associated with incomplete or incorrect folding (3–6).

Previous studies on the conformational effects of protein glycosylation have principally relied upon NMR (7–9) and CD spectroscopy (10, 11). However, these methods present some limitations when considering the conformational dynamics of flexible peptides. Specifically, the time frame of NMR measurements is such that conformational averaging could obscure specific effects of glycosylation on a polypeptide framework. In addition, the molecular weights of the peptides and glycopeptides under evaluation are such that rotational correlation times would greatly affect the nuclear Overhauser effect (NOE) measurements, making the comparative studies difficult (12). Although CD spectroscopy operates on a faster time scale, the technique is mostly applicable to peptides with strong spectroscopic signals, such as α-helical motifs (10). In contrast, fluorescence energy transfer (FET) studies allow the assessment of specific conformational features, through the measurement of a single interprobe distance, on the same rapid time scale over which conformational fluctuations occur.

The publication costs of this article were defrayed in part by page charge payment. This article must therefore be hereby marked "*advertisement*" in accordance with 18 U.S.C. §1734 solely to indicate this fact.

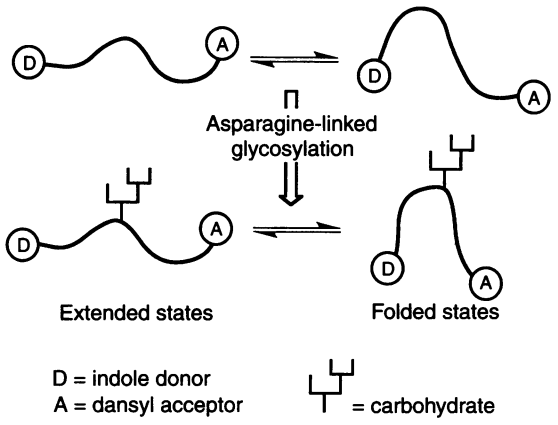

FIG. 1. Conformational dynamics of peptides and glycopeptides.

Thus, this technique provides information that is complementary to that obtained from other spectroscopic methods (13). Furthermore, the high sensitivity (μM concentrations) of fluorescence measurements and compatibility with aqueous media at neutral pH make this method valuable for the study of the conformational effects of covalent protein modifications (Fig. 1).

The current studies are targeted at establishing physical methods for assessing the impact of glycosylation on peptide conformational dynamics. We describe FET studies on three oligopeptides. The peptide sequences were selected from glycoproteins for which a high resolution x-ray structure was available. The peptides and corresponding glycopeptides, prepared through enzyme-catalyzed glycosylation, incorporate indole (donor) and 5-(dimethylamino)naphth-1-ylsulfonyl [dansyl (Dns); acceptor] fluorophores. Steady-state and time-resolved fluorescence measurements of both fluorophores are described. In time-resolved measurements, the donor decays have been analyzed for the effects of energy transfer to provide distributions of interprobe distances and, thus, reveal information on the peptide conformation. When examined in aqueous solution, two of the peptide sequences, which are found in β-turn conformations in the native glycoprotein (14), were seen to adopt more compact, folded conformations upon glycosylation.

MATERIALS AND METHODS

Synthesis of Fluorescently Labeled Peptides. The basic sequences of the peptides examined are derived from hemag-

Abbreviations: FET, fluorescence energy transfer; Dol-PP-GlcNAc-GlcNAc, dolichylpyrophosphoryl-*N*,*N*′-diacetylchitobiose; dansyl and Dns, 5-(dimethylamino)naphth-1-ylsulfonyl-; R_0, distance of 50% transfer efficiency; Q_0, quantum yield. Peptide sequences are represented with the standard one- and three-letter codes, including O and Orn to represent ornithine.

*To whom reprint requests should be addressed.

glutinin (14) and the Fab fragment of immunoglobulin A (IgA) (15). The sequences AVPNGTLV and ITPNGSI are taken from residues A19–A26 and A282–A288 of hemagglutinin. The sequence SGTMNVTWGK is taken from residues H151–H160 of IgA Fab J539. Peptides **1**, **2**, and **3** incorporate both the donor (indole) and acceptor (dansyl) chromophore. Peptides **4**, **5**, **6**, and **7** incorporate only the donor chromophore for control studies. All peptides were capped at carboxyl and amino termini to emulate internal peptide sequences. Peptides were as follows (underlined residues are those identical with the original protein sequence): **1**, Ac-Orn(δDns)-Ala-Val-Pro-Asn-Gly-Thr-Trp-Val-NH_2; **2**, Ac-Orn(δDns)-Ile-Thr-Pro-Asn-Gly-Thr-Trp-Ala-NH_2; **3**, Dns-Ser-Gly-Thr-Met-Asn-Val-Thr-Trp-Gly-Lys-NH_2; **4**, Ac-Orn-Ala-Val-Pro-Asn-Gly-Thr-Trp-Val-NH_2; **5**, Ac-Orn-Ile-Thr-Pro-Asn-Gly-Thr-Trp-Ala-NH_2; **6**, Ac-Ser-Gly-Thr-Met-Asn-Val-Thr-Trp-Gly-Lys-NH_2; **7**, Ac-Orn(δAc)-Ala-Val-Pro-Asn-Gly-Thr-Trp-Val-NH_2.

Peptides were synthesized using standard 9-fluorenylmethoxycarbonyl (FMOC) chemistry on a Milligen model 9050 peptide synthesizer, with either PAL or PAL-PEG resins to produce C-terminal amides. N-terminal dansyl (Dns) and acetyl (Ac) derivatives were formed while the peptide was still bound to the resin by using either acetic anhydride or dansyl chloride and triethylamine in dimethylformamide. Dansyl derivatization of ornithine in acetyl-capped peptides was effected after peptide cleavage from the solid-phase support. The peptides were cleaved from the resin by using reagent R (trifluoroacetic acid/thioanisole/ethanedithiol/anisole, 90:5:3:2) with a cleavage time of 2 hr. Peptides were purified by reverse-phase HPLC and characterized by NMR, mass spectrometry, UV absorption spectrophotometry, and fluorescence spectroscopy.

Enzymatic Glycosylation of Peptides. The glycopeptides corresponding to **1**, **2**, **3**, and **7** were prepared by oligosaccharyl transferase-catalyzed glycosylation using dolichylpyrophosphoryl-*N*,*N*′-diacetylchitobiose (Dol-PP-GlcNAc-GlcNAc) (16) as the disaccharide donor and a crude pig liver microsomal preparation for oligosaccharyl transferase activity. Dol-PP-GlcNAc-[^{3}H]GlcNAc was prepared as described previously, using low-specific-activity uridine diphospho-*N*-acetyl-D-[6-^{3}H]glucosamine (12 μCi/μmol; 1 Ci = 37 GBq) and synthetic Dol-PP-GlcNAc. The resulting glycosylated peptides were therefore modified with a truncated disaccharide representing part of the carbohydrate normally transferred *in vivo* (15). Glycopeptide products were exhaustively purified by sequential processes including gel filtration (Bio-Rad P4) and reverse-phase HPLC (C_{18}) chromatography. The glycopeptides were characterized via several independent methods. In all cases the glycopeptides had identical absorption spectra and quantitatively similar fluorescence emission spectra to the corresponding peptides, indicating that they contained both indole and dansyl chromophores. The products were ^{3}H-labeled with good efficiency on the basis of radiolabeled starting material (80–90% in the crude products and 30–40% after multistep purification). Each glycopeptide eluted earlier than the corresponding peptide on gel-filtration chromatography (Bio-Rad P4), indicating the higher molecular weight of the modified peptide. In all cases, glycopeptides eluted before the corresponding peptides on reverse-phase HPLC: (C_{18}; 0.46 × 15 cm), flow rate 1 ml/min, 0–5 min 100% H_2O containing 0.1% trifluoroacetic acid, followed by a linear gradient to 40% CH_3CN containing 0.08% trifluoroacetic acid over 25 min. Peptide data were as follows: **1**, peptide 30.0 min and glycopeptide 29.4 min; **2**, peptide 26.3 min and glycopeptide 25.6 min; **3**, peptide 29.5 min and glycopeptide 25.5 min; **7**, peptide 24.1 min and glycopeptide 23.1 min.

Steady-State Fluorescence and UV Measurements. Steady-state fluorescence measurements were made by using an SLM Aminco model 500 fluorometer. UV absorbances were measured using a Shimadzu model UV160 spectrophotometer. In both cases, the data were transferred to an IBM personal computer-compatible computer, for manipulation. Steady-state emission spectra of the dansyl fluorophore were measured in water and water/acetonitrile, 1:1 for both peptides and glycopeptides to investigate the effects of a more hydrophobic solvent environment. The distance of 50% transfer efficiency (R_0) was calculated from steady-state donor fluorescence and absorption spectra, with dansyl-asparagine used as an absorbance standard for the dansyl group, and these peptides in the appropriate solvents, used as the emission standard (17, 18). Quantum yields (Q_0) were determined from the emission spectra in comparison with tryptophan in water, which has been reported as 0.14 (17).

Time-Resolved Fluorescence Measurements. Time-resolved fluorescence intensity measurements were made on a time-correlated single-photon-counting apparatus. In this technique, a 15-ps laser pulse is applied to the sample, and the emission is detected by counting single-photon pulses on a photomultiplier tube. Laser pulses were generated on a cavity-dumped dye laser, which was pumped by a mode-locked Nd-yttrium/aluminum garnet laser. These pulses were then frequency doubled with a tunable β-barium borate crystal. Fluorescence was monitored at a 90° angle through a monochromator with a fast photomultiplier tube. Tryptophan signals were monitored at 390 nm, and dansyl signals were observed at 550 nm. Donor lifetimes in the absence of acceptor were analyzed as a sum of exponential decays,

$$I = \sum_{i=1,n} \alpha_i e^{-\frac{t}{\tau_i}}, \qquad [1]$$

convoluted with the instrument response function. Nonlinear least-squares curve fitting gave the appropriate lifetimes and preexponential factors. Acceptor lifetimes were determined similarly, by using decays generated by excitation at 325 nm to excite the acceptor alone. The instrument response function is measured as the response to the directly observed laser pulse. Time-resolved measurements for all peptides and glycopeptides were done in both water and water/acetonitrile, 1:1 mixtures, to correspond with the steady-state measurements.

Analysis of Fluorescence Decays. The probability of energy transfer between a donor and an acceptor depends upon the inverse sixth power of the distance between them. The rate of FET is described by:

$$n_{D\to A} = \frac{1}{\tau}\left(\frac{R_0}{r}\right)^6. \qquad [2]$$

R_0, the distance of 50% transfer is determined as $R_0 = (J\kappa^2 Q_0 n^{-4})^{1/6} \times 9.7 \times 10^3$ Å (18). κ^2, the orientation factor, is assumed to be 2/3 for random orientation, n is the refractive index and was obtained from reference tables, Q_0 is the quantum yield of the donor in the absence of the acceptor, and J, the overlap integral, is defined as

$$J = \frac{\int F(\lambda)\varepsilon(\lambda)\lambda^4 d\lambda}{\int F(\lambda) d\lambda}, \qquad [3]$$

where $F(\lambda)$ is the fluorescence of the donor in arbitrary units; $\varepsilon(\lambda)$ is the extinction coefficient of the acceptor in $cm^{-1}\cdot M^{-1}$, and λ is in cm. These integrals were carried out over the whole range of the tryptophan emission, from 300–450 nm. Due to the flexible and dynamic nature of the oligopeptides under evaluation, the systems are not well modeled by a single, fixed donor–acceptor distance. Therefore, to relate the fluorescence decay of a donor–acceptor pair to the distribution of distances between them, including the effects of diffusion, the following differential equation must be solved (13):

$$\frac{\partial \bar{N}(r,t)}{\partial t} = \left(\frac{1}{\tau}\left[1 + \left(\frac{R_0}{r}\right)^6\right]\right)\bar{N}(r,t) + \frac{1}{N_0(r)}\frac{\partial}{\partial r}\left[N_0(r)D(r)\frac{\partial \bar{N}(r,t)}{\partial r}\right], \quad [4]$$

where $N_0(r)$ is the initial distribution of the population as a function of the donor–acceptor distance and $\bar{N}$ (r,t) is the remaining normalized excited-state molecules as a function of donor–acceptor distance and time. This differential equation can be solved forward in time to give $\bar{N}$ (r,t). The impulse decay (i_D) of the donor can then be calculated by multiplying with $N_0(r)$, integrating over r, and then convoluting with the instrument response function to generate a full decay (13). Distributions were calculated as a weighted Gaussian, using the equation (19, 20):

$$N_0(r) = 4\pi c r^2 e^{(-a(r-b)^2)}, \quad [5]$$

where a, b, and c are adjustable parameters, corresponding to the width, center, and scale of the distribution. Bimodal distributions were calculated using a sum of two Gaussian distributions. Nonlinear least-squares fitting of these curves to the observed decays by the Marquardt–Levenberg algorithm allows us to calculate the appropriate parameters. Routines for curve fitting, singular value decomposition, and Fourier convolution were provided by ref. 21. Bimodal distance distributions were necessary, as unimodal distance distributions yielded unsatisfactory fits (χ^2_R between 6 and 10) (22).

Because tryptophan has an intrinsically heterogenous decay and required a biexponential fit, $i_D(t)$ was calculated individually for each donor lifetime, and then the appropriately weighted sum was used in further calculations.

RESULTS

Three peptides, **1**, **2**, and **3**, were selected for study, based on sequences of glycoproteins with known crystal structures in which the ultimate glycosylated sequence has a very distinct conformation. The sequences selected exemplify two β-turn motifs (**1** and **2**), from the structure of hemagglutinin A (23), and one strand of a β-sheet structure (**3**), from the Fab fragment of IgA (15). The β-turn is of considerable interest because this motif has been previously identified as a common feature of glycosylation sites (24) and is a potential structural nucleation element in protein folding (25). In addition, this motif can produce large changes to a single interprobe distance and so is well-suited to the FET technique. The sequences were modified to allow for the incorporation of two fluorescent chromophores, the dansyl and the indole moiety, on either side of the glycosylated region. The R_0 of this pair of chromophores, at 17–19 Å, is appropriate for these sequences, as the interprobe distance can vary from <9–30 Å, depending upon conformation. Additionally, the donor-only peptides, **4**, **5**, **6**, and **7**, were prepared for evaluation of the indole fluorescence behavior in the absence of acceptor (dansyl) chromophore.

Table 1. Analysis of tryptophan fluorescence parameters for peptides **4**, **5**, and **6**

Peptide	Solvent	α	τ, ns	χ^2R	Q_0	R_0, Å
4	H_2O	0.29	0.60	2.0	0.16	19.9
		0.71	3.37			
5	H_2O	0.35	0.91	2.0	0.08	18.2
		0.65	3.11			
6	H_2O	0.52	2.39	2.1	0.06	17.4
		0.48	0.38			
4	H_2O/CH_3CN, 1:1	0.49	1.43	1.7	0.15	19.8
		0.51	3.52			
5	H_2O/CH_3CN, 1:1	0.48	1.53	1.3	0.14	19.8
		0.52	3.54			
6	H_2O/CH_3CN, 1:1	0.38	2.52	2.3	0.12	19.3
		0.62	0.27			

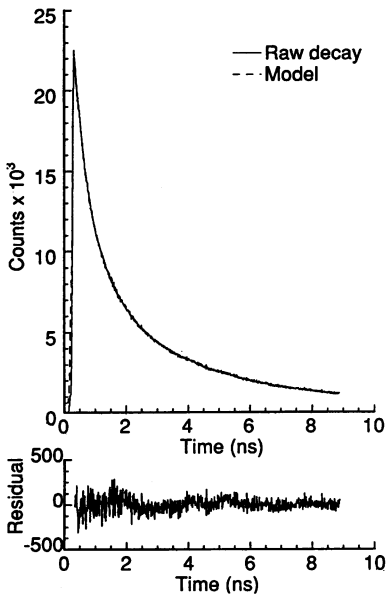

FIG. 2. Typical donor emission-decay curve and the corresponding dynamic analysis curve fit.

Steady-State Fluorescence Emission Measurements and Donor Emission Characterization. Steady-state fluorescence spectra demonstrate that the tryptophan emission is heavily quenched in the presence of acceptor and that acceptor emission is enhanced in these cases, indicating that energy transfer is occurring. Tryptophan emission data for peptides **4**, **5**, and **6**, including the quantum yield Q_0 and R_0, as obtained from steady-state fluorescence, and the exponential-fit parameters α, τ, and χ^2, as obtained from time-resolved fluorescence of the donor-only peptides are summarized in Table 1.

Distance Distribution Analysis of Donor Emission Decays. Initial analysis of the tryptophan donor decays showed that there were significant differences between the decays observed for glycopeptides and those of the unglycosylated peptides. Previously, donor–acceptor distances have often been estimated from the lifetimes recovered in an exponential analysis (18, 26). The dynamic distribution model described above allows for a more direct interpretation of donor-emission decays into a physical model of donor–acceptor distances (13, 19, 22, 27, 28). Fourteen of the sixteen curve fits had χ^2_R values between 1.1 and 2.0, whereas the other two were 3.5. Fig. 2 shows an example of the data and the corresponding curve fit. The center and width of the shorter distance distribution were well defined by the fits, whereas the diffusion parameter, and the center and width of the longer distance distribution were less well characterized, as these distances were large compared with R_0. Steady-state fluorescence indi-

Table 2. Comparison of tryptophan fluorescence parameters for peptide **7** and its corresponding glycopeptide

Peptide	Solvent	α	τ, ns	χ^2R
Peptide **7**	H_2O	0.63	2.38	1.42
		0.37	0.96	
Glycopeptide	H_2O	0.65	2.65	1.91
		0.35	0.42	
Peptide **7**	H_2O/CH_3CN, 1:1	0.78	2.78	1.69
		0.22	0.44	
Glycopeptide	H_2O/CH_3CN, 1:1	0.57	2.79	1.99
		0.43	0.38	

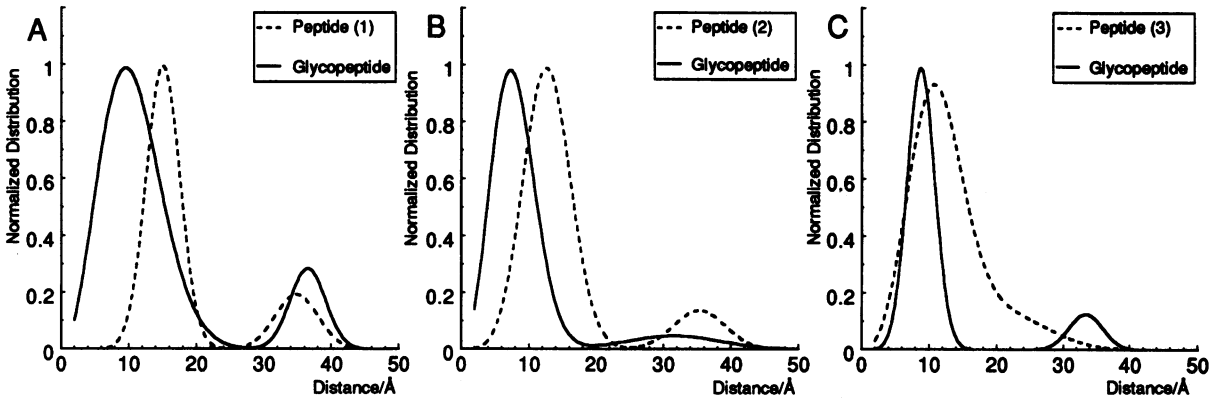

FIG. 3. Dynamic distribution plots for peptides and glycopeptides in water. (*A*) Ac-Orn(δDns)-Ala-Val-Pro-Asn-Gly-Thr-Trp-Val-NH_2 (**1**). (*B*) Ac-Orn(δDns)-Ile-Thr-Pro-Asn-Gly-Thr-Trp-Ala-NH_2 (**2**). (*C*) Dns-Ser-Gly-Thr-Met-Asn-Val-Thr-Trp-Gly-Lys-NH_2 (**3**).

cated that at the concentration ranges observed, there was no observable intermolecular energy transfer.

Potential Carbohydrate–Fluorophore Interactions. If the carbohydrate of the glycopeptides interacted with the fluorophores and affected their fluorescence, this could seriously complicate interpretation of the fluorescence-decay data. Studies of the tryptophan decay in peptide **7** and the corresponding glycopeptide, containing only the donor chromophore, show no significant effects upon the observed tryptophan decay. This result indicates that the changes observed in peptides containing the acceptor are due to conformational changes in the backbone of the molecule and not to specific interactions between the tryptophan and the carbohydrate groups. These data are summarized in Table 2. Similarly, measurements of the dansyl chromophore quantum yield and emission λ_{max}, both of which are highly sensitive to the environment of the dansyl group, show no significant differences within any peptide/glycopeptide pair. For example, for **1**, the fluorescence properties observed are as follows: peptide (Q 0.063, emission λ_{max}, 562 nm), glycopeptide (Q 0.063, emission λ_{max}, 562 nm). If a dansyl–carbohydrate interaction were present, sufficient to significantly affect the conformation of the molecule, distinct changes in the dansyl environment would be predicted, which would be reflected in these parameters.

DISCUSSION

Peptide Conformational Distributions in Water. Distance distribution data for peptides and glycopeptides **1**, **2**, and **3** in water are illustrated in Fig. 3. In this medium, significant conformational effects of glycosylation are observed. For peptides **1** and **2**, a large decrease in the average interchromophore distance of the primary peptide population is seen upon glycosylation. The average distance drops from 14.8 Å to 9.5 Å for peptide **1** (Fig. 3*A*) and from 12.4 Å to 7.7 Å for peptide **2** (Fig. 3*B*). In these two cases, there is only a small change in the fraction of the population at long distances. The dynamic distribution data for peptide **3** (Fig. 3*C*) are distinct. In this case there is little shift in the interchromophore distance (9.8 Å vs. 8.8 Å) of the compact population; however, on glycosylation the population distributions narrow. The data presented are very significant in the context of the ultimate structure adopted by each sequence in the glycosylated proteins. For sequences **1** and **2**, the structure of the final folded protein locates the glycosylated asparagines at position (i + 2) of reverse-turn motifs, with the flanking sequences in a β-hairpin structure. The shift of interchromophore distances seen with the FET studies reflects the development of a more compact structure of this type (Cα—Cα distance in a typical β-hairpin structure is ≈7 Å). In contrast, the polypeptide sequence after which peptide **3** is patterned adopts an extended structure in the protein architecture but would be expected to be unstructured in solution. The much smaller changes observed here indicate that glycosylation does not significantly induce formation of a compact, turn-type conformation in this peptide.

Peptide Conformational Distributions in Nonpolar Solvents. Time-resolved fluorescence spectra were also collected in acetonitrile/water, 1:1. Spectra taken in this system show two consistent trends in the dynamics analysis, as illustrated in Fig. 4. (*i*) There is a significant increase (up to 30–40% total) in the longer distance distribution for both peptides and glycopeptides. (*ii*) For peptides **1** and **2** there is no significant shift in the interprobe distance upon glycosylation. These

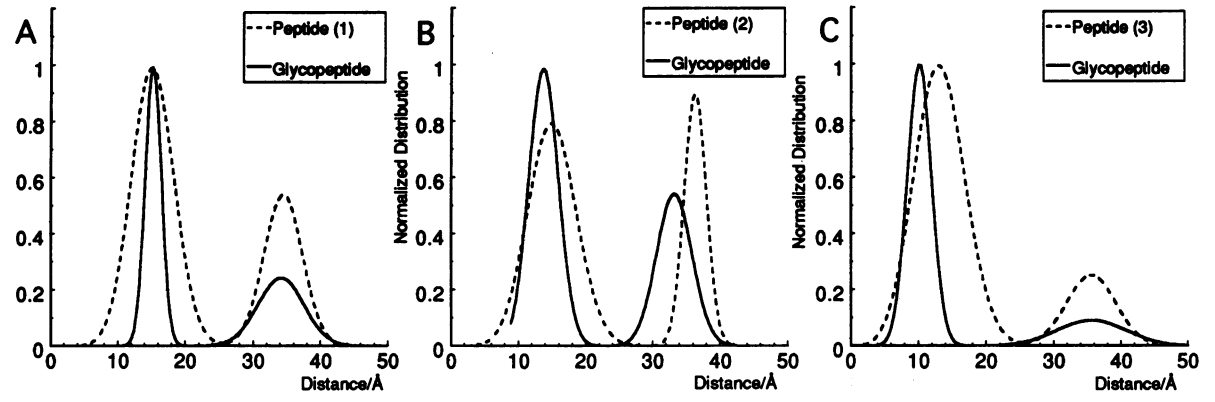

FIG. 4. Dynamic distribution plots for peptides and glycopeptides in water/acetonitrile, 1:1. (*A*) Ac-Orn(δDns)-Ala-Val-Pro-Asn-Gly-Thr-Trp-Val-NH_2 (**1**). (*B*) Ac-Orn(δDns)-Ile-Thr-Pro-Asn-Gly-Thr-Trp-Ala-NH_2 (**2**). (*C*) Dns-Ser-Gly-Thr-Met-Asn-Val-Thr-Trp-Gly-Lys-NH_2 (**3**).

results demonstrate that, in general, the peptides are less folded in nonpolar solvents than in water, indicating that the major impetus for folding into a compact conformation may be due to hydrophobic effects. Furthermore, glycosylation seems to have a relatively small effect upon conformational parameters in this solvent system. The additional data from acetonitrile/water studies provide a point of reference for comparison to the aqueous media data and suggest that the conformational changes observed on peptide glycosylation are driven to a large extent by the nature of the surrounding medium.

The structural and functional integrity of many proteins relies on specific co- and posttranslational protein-modification reactions. Asparagine-linked protein glycosylation may serve many diverse roles. Some proteins require N-linked oligosaccharides to maintain proper function (7, 29) or to be correctly targeted (1). In other cases, the presence or absence of the oligosaccharide seems to make no difference to the function of the native protein (30). It is known, however, that N-linked glycosylation occurs cotranslationally (31, 32) and has the potential to affect the course of protein folding. For hemagglutinin and immunoglobulin A it is established that glycosylation serves a vital role in the folding and assembly of viable proteins (4–6). The studies described here specifically indicate that glycosylation can alter the conformational profile of a polypeptide and allow it to sample conformational space not originally accessible to it. Therefore, this result implies that the glycosylation event could serve to funnel the nascent polypeptide structure through a particular pathway for folding. In the absence of glycosylation, specific folded intermediates would be inaccessible, and the outcome would be a delinquent protein product. Protein folding occurs extremely rapidly (33), and the timely formation of structural nucleation elements, triggered by glycosylation as the polypeptide is biosynthesized, may be one way to assist in proper protein folding, thus avoiding opportunities for interaction with unfolded proteins and aggregation. An understanding of the various ways in which N-linked glycosylation influences protein folding will be important both for understanding the general significance of glycosylation and for understanding folding pathways for glycoproteins. As demonstrated in this study, the time scale of FET measurements makes this a valuable technique for probing intramolecular distances in flexible peptides and the changes in conformational dynamics associated with protein-modification reactions.

We are grateful to Chris Kenyon and Dr. Jay Winkler of the Beckman Institute Laser Resource Center for the use of the time-correlated single-photon-counting apparatus and for invaluable technical assistance. The Laser Resource Center is supported by the Arnold and Mabel Beckman Foundation. This research was supported by National Institutes of Health grant GM 39334 and a Fannie and John Hertz predoctoral fellowship (to K.W.R.). B.I. also acknowledges support from the Alfred P. Sloan Foundation, the Camille and Henry Dreyfus Teacher Scholar Program, the Lilly Grantee Program, and Zeneca Pharmaceuticals. This paper is contribution no. 8981 from the Division of Chemistry and Chemical Engineering, California Institute of Technology.

1. Pfeffer, S. R. & Rothman, J. E. (1987) *Annu. Rev. Biochem.* **56,** 829–852.
2. Rowling, P. J. E. & Freedman, R. B. (1993) in *Subcellular Biochemistry: Endoplasmic Reticulum*, eds. Borgese, N. & Harris, J. R. (Plenum, New York), pp. 41–80.
3. Riederer, M. A. & Hinnen, A. (1991) *J. Bacteriol.* **173,** 3539–3546.
4. Marquardt, T. & Helenius, A. (1992) *J. Cell Biol.* **117,** 505–513.
5. Hickman, S., Kulczycki, A. J., Lynch, R. G. & Kornfeld, S. (1977) *J. Biol. Chem.* **252,** 4402–4408.
6. Copeland, C. S., Zimmer, K.-P., Wagner, K. R., Healey, G. A., Mellman, I. & Helenius, A. (1988) *Cell* **53,** 197–209.
7. Joao, H. C., Scragg, I. G. & Dwek, R. A. (1992) *FEBS Lett.* **307,** 343–346.
8. Wormald, M. R., Wooten, E. W., Bazzo, R., Edge, C. J., Feinstein, A., Rademacher, T. W. & Dwek, R. A. (1991) *Eur. J. Biochem.* **198,** 131–139.
9. Davis, J. T., Hirani, S., Bartlett, C. & Reid, B. R. (1994) *J. Biol. Chem.* **269,** 3331–3338.
10. Otvos, L., Thurin, J., Kollat, E., Urge, L., Mantsch, H. M. & Hollosi, M. (1991) *Int. J. Pept. Protein Res.* **38,** 476–482.
11. Aubert, J. P., Helbecque, N. & Loucheux-Lefebvre, M. H. (1981) *Arch. Biochem. Biophys.* **208,** 20–29.
12. Bothner-By, A. A., Stephens, R. L., Lee, J., Warren, C. D. & Jeanloz, R. W. (1984) *J. Am. Chem. Soc.* **106,** 811.
13. Beechem, J. M. & Haas, E. (1989) *Biophys. J.* **55,** 1225–1236.
14. Wilson, I. A., Skehel, J. J. & Wiley, D. C. (1981) *Nature (London)* **289,** 366–373.
15. Suh, S. W., Bhat, T. N., Navia, M. A., Cohen, G. H., Rao, D. N., Rudikoff, S. & Davies, D. R. (1986) *Proteins Struct. Funct. Genet.* **1,** 74–80.
16. Imperiali, B. & Zimmerman, J. W. (1990) *Tetrahedron Lett.* **31,** 6485–6488.
17. Schiller, P. W. (1972) *Proc. Natl. Acad. Sci. USA* **69,** 975–979.
18. Stryer, L. (1978) *Annu. Rev. Biochem.* **47,** 819–846.
19. Beals, J. M., Haas, E., Krausz, S. & Scheraga, H. A. (1991) *Biochemistry* **30,** 7680–7692.
20. Haas, E., Wilcheck, M., Katchalski-Katzir, E. & Steinberg, I. (1975) *Proc. Natl. Acad. Sci. USA* **72,** 1807–1811.
21. Press, W. H., Teukolsky, S. A., Vetterling, W. T. & Flannery, B. P. (1992) *Numerical Recipes in C* (Cambridge Univ. Press, Cambridge, U.K.).
22. Wu, P., Rice, K. G., Brand, L. & Lee, Y. C. (1991) *Proc. Natl. Acad. Sci. USA* **88,** 9355–9359.
23. Wilson, I. A., Ladner, R. C., Skehel, J. J. & Wiley, D. C. (1983) *Biochem. Soc. Trans.* **11,** 145–147.
24. Beintema, J. J. (1986) *Biosci. Rep.* **6,** 709–714.
25. Wright, P. E., Dyson, H. J. & Lerner, R. A. (1988) *Biochemistry* **27,** 7167–7175.
26. Johnson, D. A., Leathers, V. L., Martinez, A.-M., Walsh, D. A. & Fletcher, W. H. (1993) *Biochemistry* **32,** 6402–6410.
27. Eis, P. S. & Lakowicz, J. R. (1993) *Biochemistry* **32,** 7981–7993.
28. Maliwal, B. P., Lakowicz, J. R., Kupryszewski, G. & Rekowski, P. (1993) *Biochemistry* **32,** 12337–12345.
29. Rudd, P. M., Joao, H. C., Coghill, E., Fiten, P., Saunders, M. R., Opdenakker, G. & Dwek, R. A. (1994) *Biochemistry* **33,** 17–22.
30. Paulson, J. C. (1989) *Trends Biochem. Sci.* **14,** 272–276.
31. Bergman, L. W. & Kuehl, W. M. (1978) *Biochemistry* **17,** 5174–5180.
32. Kiely, M. L., McKnight, G. S. & Schimke, R. T. (1976) *J. Biol. Chem.* **251,** 5490–5495.
33. Matthews, C. R. (1993) *Annu. Rev. Biochem.* **62,** 653–683.